Carbohydrate Polymers 88 (2012) 165–172

Contents lists available at SciVerse ScienceDirect

Carbohydrate Polymers

journal homepage: www.elsevier.com/locate/carbpol

Improved flexibility of thermally stable poly-lactic acid (PLA)

Jeremy Hughes, Ron Thomas*, Youngjae Byun, Scott Whiteside

Department of Packaging Science, Clemson University, B-212 Poole & Agricultural Center, Clemson, SC 29643-0320, USA

ARTICLE INFO

Article history:
Received 12 October 2011
Accepted 25 November 2011
Available online 6 December 2011

Keywords:
Polylactic acid (PLA)
Solvent
Flexibility
Crystal structure

ABSTRACT

The objective of this research was to determine the optimum solvent mixture ratio to improve flexibility while maintaining the thermal expansion stability of PLA film. PLA films were produced from mixed solvent solutions of (M: methylene chloride) and (A: acetonitrile) and 10% plasticizer using the solvent-casting technique. The ratio of solvents used were 70% methylene chloride with 30% acetonitrile (73MA10), 60% methylene chloride with 40% acetonitrile (64MA10) and 50% methylene chloride with 50% acetonitrile (55MA10). The single solvent solution was 100% methylene chloride (100M10). Thermal stability was enhanced by the addition of acetonitrile. Thermal stability of 55MA10 was 0.6219 μm/°C as compared to 15.63 μm/°C for 100M10. Increased concentration of acetonitrile also improved crystal formation as seen by the peak intensity of WAXD. Films that had more crystallinity (64MA10, 55MA10), had less thermal expansion stability and brittle behavior. In contrast, 73MA10 having less crystallinity, had the best flexibility at 49.36% elongation while having similar thermal behavior as the more crystalline films. This work shows that PLA film produced by solvent casting from solvent mixture compared to a traditional single solvent will have better thermal and mechanical performance.

1. Introduction

Poly (lactic acid) (PLA) is an aliphatic thermoplastic, compostable, biocompatible polymer derived from starch contained in products like corn, sugar cane and sugar beets (Garlotta, 2001). For the past several years PLA has been used in the biomedical field for implant applications and wound dressing (Mano, Gomez-Ribelles, Alves, & Salmeron-Sanchez, 2005). With the advance of new technologies and lower processing costs, PLA is being used in other commodity areas like packaging, textiles and composite materials (Drmright, Gruber, & Henton, 2000). With respect to packaging, PLA has certain limitations. Low deformation at break, low heat resistance, high modulus, hydrophilic properties and brittle behavior are factors that limit PLA from being a serious material in the packaging industry (Drmright et al., 2000; Rhim, Hong, & Ha, 2009; Sin-Lin, Zhi-Hua, Yang, & Yang, 2008).

The use of PLA in packaging has primarily been for rigid packaging due to its poor mechanical properties as a thin material (Pillin, Montrelay, & Grohens, 2006). The solvent-casting technique is a widely used technique in research used to produce thin biopolymer films (Pezzin, Alberda, Zavaglia, Ten Brinke, & Duek, 2003). PLA is known to be highly soluble in solvents such as methylene chloride, benzene, chloroform, and dioxane (Furuhashi, Wakuda, & Yoshie, 2006; Pillin et al., 2006). Each solvent influences film properties differently. For instance, chloroform induces a greater chain mobility of the polymer and dioxane causes a rough surface of the film due to its slow evaporation rate (Bistac & Schultz, 1997; Haidong, Wei, Chao, Xuesi, & Xiangling, 2009). Previous research involving solvent-casting has focused on increasing the crystallinity of thin PLA film to improve thermal stability using various solvent mixtures, but this in turn diminished its mechanical ability (Byun et al., 2011). This inability to behave ductile limits the practical use of PLA as a thin film. Solvent-casting involves dissolving a resin polymer into a solvent such as methylene chloride, chloroform and benzene and then casting it into a thin wet film to dry (Byun, Kim, & Whiteside, 2010; Furuhashi et al., 2006). The mobility of solvent molecules in a polymer solution plays a large role in the properties of the polymer (Jyh-Ping & Sung-Hwa, 2005). The solvent induced conformational changes affect the crystallinity of the polymer (Paragkumar, Edith, & Jean-luc, 2006). PLA has low solubility in solvents like toluene, acetone, acetonitrile and ethyl acetate (Paragkumar et al., 2006). Casting with a solvent like methylene chloride showed more of a polymer solvent interaction and led to good solubility (Byun et al., 2011). Huda et al. (2002) discovered that PLA solutions in methylene chloride and chloroform resulted in a random conformation of molecules. Byun et al. (2011) used PLA solutions of methylene chloride and acetonitrile and saw an intramolecular interaction of molecules leading to a polymer–polymer interaction.

Most research has focused on improving the mechanical and barrier properties of PLA by adding nanoclays and natural fibers during the making of PLA films (Rhim et al., 2009). Other researchers have looked at how to improve antimicrobial properties (Rhim et al., 2009). Although mechanical ability and barrier

* Corresponding author. Tel.: +1 864 888 7541; fax: +1 864 656 4395.
E-mail address: rthms@clemson.edu (R. Thomas).

0144-8617/$ – see front matter © 2011 Elsevier Ltd. All rights reserved.
doi:10.1016/j.carbpol.2011.11.078

properties of PLA films are being studied well, not much work is being done to improve thermal expansion stability and enhance mechanical properties of PLA films simultaneously. Preliminary studies have proven that solvents like methylene chloride and chloroform produce clear films that have good mechanical properties but poor thermal stability (Byun et al., 2011). The mixture of methylene chloride and acetonitrile together altered the crystalline structure of PLA thin films; enhancing thermal stability but the material was brittle (Byun et al., 2011). The purpose of this research was to find the optimum ratio of solvent mixtures to produce a PLA film that is both thermally stable yet ductile in behavior to be used as a packaging film.

2. Materials and methods

2.1. Materials

The PLA resin (4032D) used for this research was purchased from Nature Works, LLC (MN, USA). PLA resin constituted a 99:1 ratio of L to D oligomer. Methylene chloride was purchased from JT Baker (USA). Acetonitrile was purchased from VWR International (PA, USA) and Polyethylene glycol 400 (PEG 400) used was purchased from Sigma–Aldrich (MO, USA). All solvents used were HPLC grade.

2.2. Film preparation

Preparing the film was done using the solvent casting technique. Before casting, the PLA resin was placed into a drying oven at 35 °C for a week to remove any moisture. 30 g of PLA and 3 g of PEG 400 were dissolved into 200 mL of solvent. The mixtures were stirred for 12 h before casting. The solvents used for this study were methylene chloride (M) and acetonitrile (A). The plasticizer used was polyethylene glycol with a molecular weight of 400. The amount of plasticizer used ranged from 10 to 20%, increasing in 2% increments. The ratios of solvents used were 100% methylene chloride (100M10), 50:50 methylene chloride:acetonitrile (55MA10), 60:40 methylene chloride:acetonitrile (64MA10) and 70:30 methylene chloride:acetonitrile (73MA10). 35 mL of dope solution was cast onto a BYTAC® (Norton Performance Plastics Corporation, Wayne, NJ, USA) coated 157 mm × 356 mm glass plate which was formed utilizing a customized film applicator. The cast films were then air dried at 23 °C for 12 h. The films were then peeled off the plates and dried in an oven at 35 °C for 8 h to evaporate any residual solvent left in the film. Only film 55MA20 had a plasticizer mixture of 20% as films 64MA and 73MA produced pin holes during casting.

2.3. Mechanical properties

The tensile strength (TS), elongation at break (%*E*), and Young's modulus (ε) of the PLA films were measured using an Instron Universal Testing Machine (Model 4201, Instron Corp., Canton, MA, USA) according to the ASTM standard method D882-88. Specimen samples, 10 cm × 2.54 cm, were cut from film samples. Samples were conditioned for 48 h at 23 ± 0.5 °C and 50% RH in a constant temperature and humidity chamber before the measurement. Initial grip separation and cross-head speed were set at 5 cm and 25 cm/min, respectively. The values presented were the average of seven measurements. Stress–strain curves were generated at a grip separation of 5 cm and a cross-head speed of 12.5 mm/min.

2.4. X-ray diffraction

Wide angle X-ray diffraction patterns were recorded using a copper anode X-ray tube (Cu-K_α radiation, $\lambda = 1.5418$ Å) (Rigaku Ultima IV, Tokyo, Japan). The scanning region of the diffraction angle (2θ) was 10–30° with continuous scan mode at a scan speed of 0.200°/min. *d*-Spacing from TEM was confirmed using Bragg's Law:

$$n\lambda = 2d\sin(\theta)$$

2.5. Differential scanning calorimetry (DSC)

Differential scanning calorimetry (DSC) of PLA solvent cast films was performed on a (Model 2920 Modulated DSC, TA instrument, USA). The glass transition temperature (T_g), crystallization temperature (T_c), and melting temperature (T_m) of the PLA films were measured. Specimens weighing 6–7 mg were heated at a rate of 10 °C/min from 20 to 180 °C with a constant nitrogen flow throughout. The percentage of crystallinity (X_c) of the PLA films was calculated according to the following equation:

$$X_c\,(\%) = \frac{\Delta H_m - \Delta H_c}{\Delta H_m^c} \cdot 100$$

where $\Delta H_m{}^c$ is the enthalpy of fusion of pure crystalline PLA (93.1 J/g) (Fischer, Sterzel, Wegner, & Kolloid-Zu, 1973; Lim, Auras, & Rubino, 2008; Tingting, Yang, & Chaobin, 2010).

2.6. Thermal expansion stability

Thermal expansion stability was analyzed by a Thermomechanical Analyzer (TMA) (2940, TA instruments). The film samples for TMA were cut into strips 0.159 cm wide and 1.27 cm long. The samples were clamped on both the ends with split aluminum balls and heated from 25 to 110 °C at the rate of 10 °C/min with a constant nitrogen flow throughout.

2.7. Transmission Electron Microscope (TEM) images

All TEM images were captured using a High Resolution Transmission Electron Microscope (Hitachi H-9500) equipped with a LaB6 filament. Operation at 200 kV was used for optimum, high resolution imaging. The microscopes software calculated the *d*-spacing of crystal lattice seen in the images.

2.8. Optical properties

Haze, transparency and clarity of the PLA film were collected using a BYK Gardner Haze Gard Plus (Model 4725, Germany).

2.9. Statistical analysis

Statistical significance was determined by analysis of variance (ANOVA) using SAS (version 9.1, SAS Institute Inc., NC). Significance was defined at a level of $P < 0.05$.

3. Results and discussion

3.1. Mechanical properties

Poly ethylene glycol 400 (PEG 400) was used as the plasticizer to help enhance the mechanical properties of the PLA film and decrease T_g (Pillin et al., 2006). PEG 400 was chosen for its ability to increase mobility of PLA macromolecules, which is a large factor aiding in the crystallization kinetics of a polymer (Pillin et al., 2006). Pillin et al. (2006) showed that adding more plasticizer (PEG 400) to the film, decreased T_g. Stress–strain curves showed that PLA 73MA10 and 100MA10 behaved ductile while 55MA10 and 64MA10 were brittle (Fig. 1). This study also showed that increasing the plasticizer concentration did not always result in a stronger

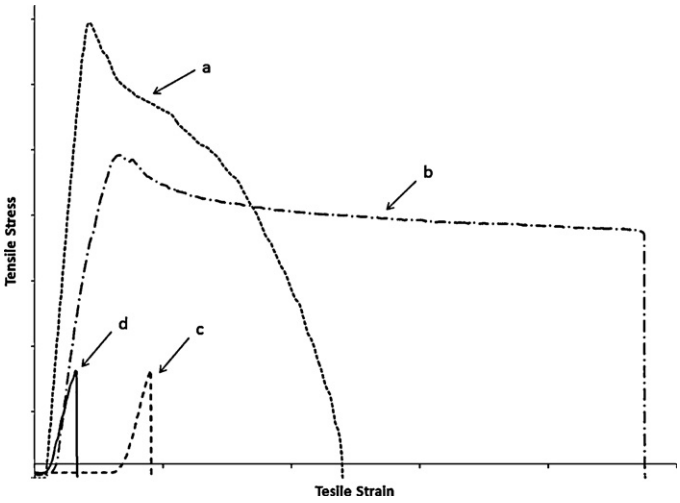

Fig. 1. Stress–strain curves of PLA film (a) 100M10; (b) 73MA10; (c) 64MA10; and (d) 55MA10.

film, with the exception of 55MA which saw a significant increase in tensile strain (Table 1a). Comparing the 10% mixtures only, film 55MA10 and 64MA10 showed the lowest values for TS of 9.13 and 13.02 MPa, respectively. They also had the lowest % elongation (Tables 1a, 1b and 1c). 100M10 had higher TS and modulus values of 52.19 and 12.02 MPa whereas 73MA10 had a TS value of 37.65 MPa and a modulus of 9.87 MPa. The % elongation however was significantly higher for 73MA10 than any of the films tested at 49.36% (Table 1c). Previous researches have shown that spherulite size increased with increasing crystallinity making the material brittle (Park, Todo, Arakawa, & Koganemaru, 2006). The crystallinity could be the key factor in why 55MA10 and 64MA10 ruptured earlier. Crazing is an important deformation mechanism observed in amorphous polymers and appears as horizontal lines from a tension source during tensile strain (Figs. 2 and 3) (Michler & Baltá-Calleja, 2005, chap. 5). These cracks are an energy absorbing

Table 1a
Mechanical properties of 55MA PLA cast films.

PLA film	Tensile strain (MPa)	Young's modulus (MPa)	% elongation
100M10	$52.19 \pm 7.52_1{}^{a}$	$12.02 \pm 1.97_1{}^{a}$	$14.24 \pm 10.37_2{}^{a}$
55MA10	$9.13 \pm 1.03_3{}^{d}$	$2.96 \pm 0.40_3{}^{d}$	$3.20 \pm 0.67_2{}^{b}$
55MA12	9.70 ± 0.67^{d}	2.87 ± 0.42^{d}	3.61 ± 0.67^{b}
55MA14	18.13 ± 2.78^{b}	7.32 ± 1.29^{b}	2.50 ± 0.29^{b}
55MA16	$12.17 \pm 3.83^{c,d}$	5.29 ± 1.06^{c}	2.25 ± 0.41^{b}
55MA18	$15.86 \pm 3.71^{b,c}$	$6.21 \pm 1.14^{b,c}$	2.55 ± 0.30^{b}
55MA20	14.05 ± 0.72^{c}	1.24 ± 0.22^{e}	2.82 ± 0.25^{b}

Different letters and subscript numbers within the same column are significantly different ($P < 0.05$).
Results are expressed as the mean ± SD ($n = 7$).
Subscript numbers are differences among 10% plasticizer only.

Table 1b
Mechanical properties of 64MA PLA cast films.

PLA film	Tensile strain (MPa)	Young's modulus (MPa)	% elongation
100M10	52.19 ± 7.52^{a}	12.02 ± 1.97^{a}	14.24 ± 10.37^{a}
64MA10	$13.02 \pm 1.64_3{}^{b}$	$3.93 \pm 0.80_3{}^{b}$	$3.51 \pm 0.81_2{}^{b}$
64MA12	7.74 ± 2.53^{c}	2.89 ± 1.12^{b}	2.78 ± 0.61^{b}
64MA14	$4.67 \pm 0.79^{c,d}$	1.68 ± 0.35^{c}	2.75 ± 0.33^{b}
64MA16	2.26 ± 0.47^{d}	1.07 ± 0.29^{c}	2.01 ± 0.37^{b}
64MA18	$4.57 \pm 1.10^{c,d}$	1.72 ± 0.35^{c}	2.66 ± 0.36^{b}

Different letters and subscript numbers within the same column are significantly different ($P < 0.05$).
Results are expressed as the mean ± SD ($n = 7$).
Subscript numbers are differences among 10% plasticizer only.

Table 1c
Mechanical properties of 73MA PLA cast films.

PLA film	Tensile strain (MPa)	Young's modulus (MPa)	% elongation
100M10	52.19 ± 7.52^{a}	12.02 ± 1.97^{a}	14.24 ± 10.37^{a}
73MA10	$37.65 \pm 2.70_2{}^{b}$	$9.87 \pm 0.60_2{}^{b}$	$49.36 \pm 22.89_1{}^{b}$
73MA12	37.02 ± 1.90^{b}	9.81 ± 0.68^{b}	27.41 ± 26.27^{b}
73MA14	31.89 ± 2.38^{d}	7.79 ± 0.82^{c}	21.20 ± 18.69^{b}
73MA16	$35.53 \pm 2.24^{b,d}$	9.55 ± 0.59^{b}	27.23 ± 22.18^{b}
73MA18	33.29 ± 3.07^{d}	8.98 ± 0.78^{b}	12.70 ± 9.45^{b}

Different letters and subscript numbers within the same column are significantly different ($P < 0.05$).
Results are expressed as the mean ± SD ($n = 7$).
Subscript numbers are differences among 10% plasticizer only.

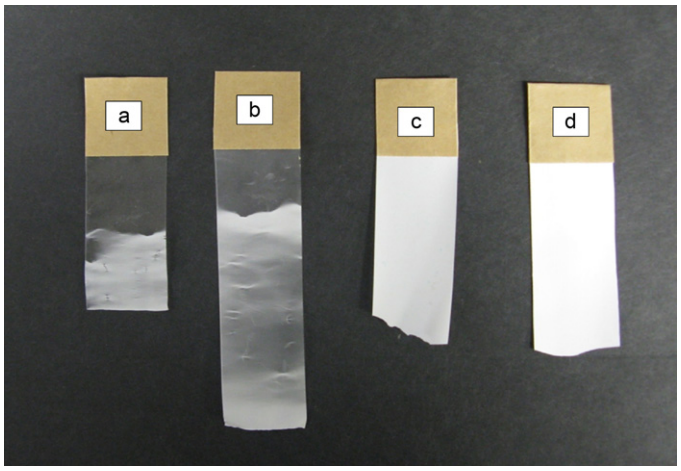

Fig. 2. Tensile specimens after testing (a) 100M10; (b) 73MA10; (c) 64MA10; and (d) 55MA10.

mechanism and increased fracture energy is accelerated by these cracks (Miller, 1996, chap. 7). At this point the tie molecules have been stretched to their limit, hydrogen bonds have broke and covalent bonds are beginning to yield and were seen only in 100M10 and 73MA10. Microscopic images of where the transparent amorphous region ends and the white (crazing) region begin can also be seen (Fig. 3). The effect of increased flexibility can be seen by stress–strain curves (Fig. 1). Films 55MA10 and 64MA10 having more crystallinity had very little tensile stress and rupture at the yield point. Films 100M10 and 73MA10 showed significant stress yield with a plastic region indicated by the increase in tensile strain before rupture. Although film 100M10 saw the highest tensile stress, 73MA10 was much more flexible. Developing films with good flexibility along with good thermal stability was the main objectives of this research. Stress–strain curves with plasticizer concentrations above 10% where not shown as they did not show any difference in the shape of the curve.

3.2. Crystallinity

X-ray diffraction profiles of the cast PLA films were taken only of films with 10% plasticizer since the increase in plasticizer did not change the crystalline structure (Fig. 4). PLA film 55MA10 and 64MA10 show multiple diffraction peaks at 2θ angle 12°, 15°, 17°, 19° and 23°, indicating the presence of new crystalline structures as compared to 73MA10 and 100M10. PLA was dissolved more easily in methylene chloride than in acetonitrile. Reports showed that the formation of stereocomplex crystallization occurs when PLA is dissolved in a poor solvent due, in part, to the strong interaction in polymer chains (Sodergard & Stolt, 2002). Byun et al. (2010) discovered that acetonitrile mixed with methylene chloride may induce the production of multiple crystalline structures in PLA film

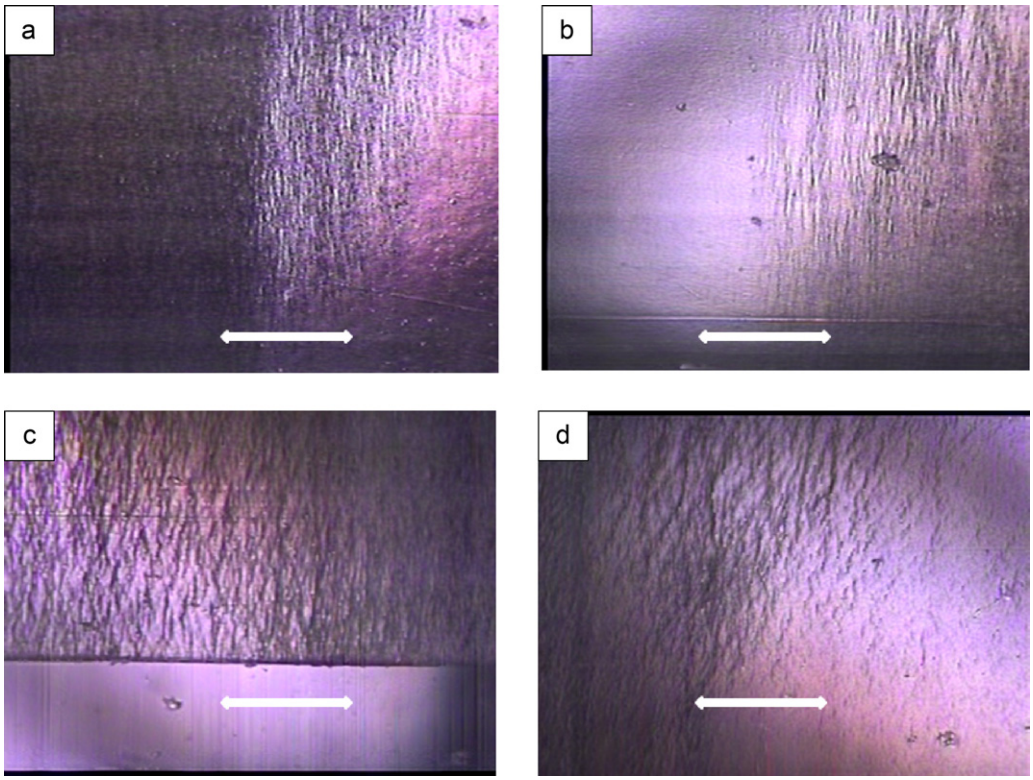

Fig. 3. Micro cracking voids of (a, c) 73MA10 and (b, d) 100M10. Arrows indicate direction film sample was pulled during tensile tests.

(Byun et al., 2011). Comparing these results with DSC data (Table 2), there was a correlation with the number of peaks and percent crystallinity. Mixing solvents with varying PLA solubility can increase the crystallinity of the film (Furuhashi et al., 2006). 55MA10 and 64MA10 having larger amounts of acetonitrile, had the highest % crystallinity and highest enthalpy of fusion for melting crystals.

Unlike 55MA10 and 64MA10, PLA film 73MA10 and 100M10 show diffraction peaks at only 17° and 19° and a small spike at 23° for 100M10. Their % crystallinity differed with 73MA10 having 31.01 and 100M10 25.99%. However, the enthalpy of fusion for melting (ΔH_m) for 100M10 and 73MA10 were more similar with 100M10 having an enthalpy of 38.95 J/g and 73MA10 with 40.12 J/g. The larger melting enthalpy for 73MA10 versus 100M10 could mean that during casting the addition of acetonitrile aided in the formation of fewer crystals not completely grown. When subjected to DSC analysis more crystals started to form before melt as indicated by the amount of energy to melt the crystal. PLA dissolved in poor solvents like acetonitrile promote more polymer–polymer interactions, in turn, leading to more crystallinity (Furuhashi et al., 2006). As for the enthalpy of crystallization (ΔH_c), only solvent mixtures of 100M10 and 73MA10 showed any energy levels (14.75 J/g and 11.25 J/g, respectively). The release of energy during this exothermic transition proves more crystalline arrangement was taking place. A larger crystallization enthalpy as with 100M10 (14.75 J/g) indicated more crystals were being arranged during heating. A lesser value or the absence of a crystallization enthalpy was conformation that crystals had already formed during casting of the film. The crystallinity of solvent cast film was also effected by solvent properties. Solvents that have high boiling points (bp) have lower rates of vaporization which leads to more time to facilitate the growth of crystals, whereas solvents with low boiling points have a higher rate of vaporization and limit the time for crystals to grow (Furuhashi et al., 2006).

Table 2
Thermal properties of solvent cast PLA films 55MA.

PLA film	T_g	T_c	T_m	ΔH_c (J/g)[a]	ΔH_m (J/g)[b]	% crystallinity
100M10	57	80	165	14.75	38.95	25.95
73MA10	58	83	165	11.25	40.12	31.01
64MA10	53		167		48.59	52.19
55MA10	55		167		53.01	56.94

[a] ΔH_c: enthalpy of crystallization.
[b] ΔH_m: enthalpy of fusion.

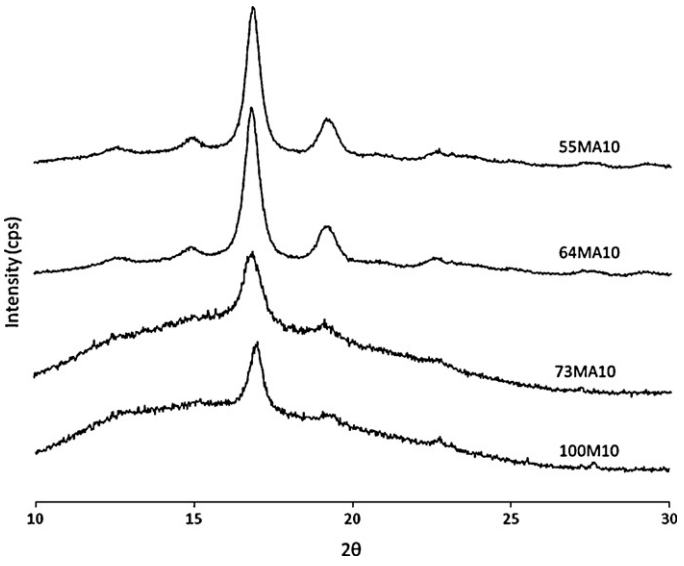

Fig. 4. Wide-angle X-ray diffraction patterns of the four different PLA films.

Poly (L-lactic acid) (PLLA) and poly (D-lactic acid) (PDLA) are isotactic and can crystallize into α, β and γ-forms (Cartier et al., 2000; De Santis & Kovacs, 1968; Hoogsten, Postema, Pennings, Ten Brinke, & Zugenmaier, 1990; Tingting et al., 2010; Xiao, Liu, & Yeh, 2010).

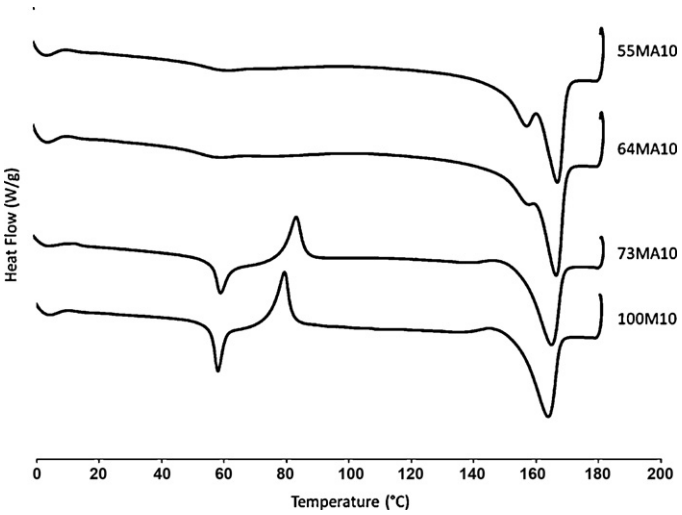

Fig. 5. DSC thermograms of the PLA films.

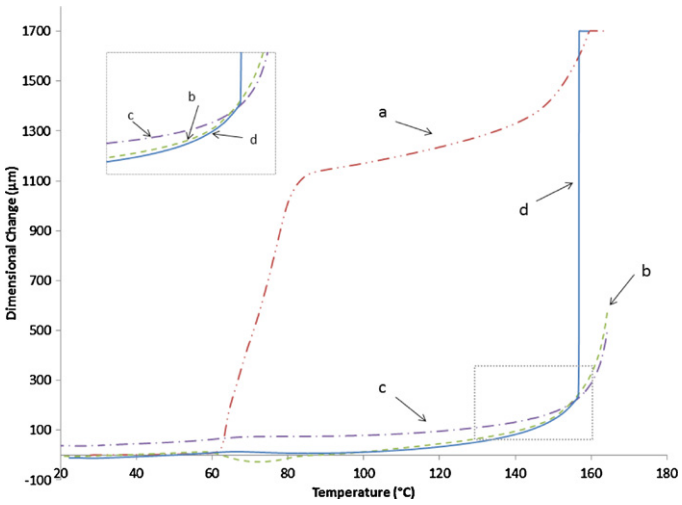

Fig. 6. TMA thermograms of the PLA films (a) 100M10; (b) 73MA10; (c) 64MA10; and (d) 55MA10.

Previous research showed that PLA undergoes a conformational change and the lowest energy conformation of a single PLLA chain is either helical 10_3 (α-form, major 2θ: 17, 19, 22) or 3_1 helices (β-form, major 2θ: 12, 25) (Bor-Kuan, Hia-Hsu, Shu-Chuan, & Antonia, 2010; Brizzolara, Cantow, Diederichs, Keller, & Domb, 1996; Slager, Brizzolara, Cantow, & Domb, 2005; Tingting et al., 2010). Jianming et al. (2005) stated that PLLA crystal structures with loose 10_3 helical chain packing are less thermally stable than the standard α form. This research proved that 73MA10 and 100M10 crystallized in the α-form due to their peak angle at 2θ 17°. However, PLA 55MA10 and 64MA10 showed small peaks at 2θ 12°, indicating a conformational change to β-form. The increase in peak width and height of 55MA10 and 64MA10 at 2θ 17° suggests that acetonitrile may increase the crystal perfection of the polymer. These more dominate peaks in 55MA10 and 64MA10 show that there were more crystalline structures than with 100M10 and 73MA10.

The X-ray diffraction peaks indicated the main crystalline features of 100M10 and 73MA10 with diffraction peaks at 17° (d = 0.2636 nm), which is an indication of α-form crystals. 55MA10 and 64MA10 saw multiple diffraction peaks, including 12° (d = 0.3708 nm), 15° (d = 0.2978 nm) and 19° (d = 0.2367) with a more intense peak at 17°. These additional peaks at angles 12°, 15° and 19° and the increase in peak intensity at 2θ 17° reveals more predominant growth of α-form polymorph and the addition of β-form crystals (Shujin, Jinglin, & Jiungau, 2008). TEM images confirmed the spacing of the lattice (Fig. 6). Overall crystallinity may have been limited due to the 99:1 ratio of L to D PLA. Previous studies have shown that adding the D form into PLLA significantly increased the crystallization of PLLA forming stereocomplex crystallites in PLLA's matrix (Hong, Cuiqing, & Muhuo, 2006; Yamane & Sasai, 2003).

3.3. Thermal properties

Films 55MA10 and 64MA10 did not show any noticeable T_c but did show T_g and T_m (Table 2 and Fig. 5). The T_g of the film is dependent upon the polymers structural arrangement and corresponds to the torsional oscillation of carbon backbone and side groups resulting in long range segmental motion above the T_g (Ahmed, Varshney, Zhang, & Ramaswamy, 2009; Selke, Culter, & Hernandez, 2004, chap. 3). The T_g's vary in curve shape and broadness (Fig. 5). The presence of crystalline structures in semi-crystalline polymers has been known to effect the glass transition resulting in a more broad transition area as compared to more amorphous polymers (Stuik, 1978). Films 55MA10 and 64MA10 showed a low sloped glass transition point versus the sharp angled peaks of the more amorphous 73MA10 and 100M10 (Fig. 5). The lack of a crystalline peak for 55MA10 and 64MA10 indicates that the polymer reached its maximum crystallinity early in the casting process. It is assumed that a double melting peak for 55MA10 and 64MA10 is attributed to the melting of multiple crystalline structures. Previous research noted that the lower temperature melting peak was attributed to the melting of subsidiary, thinner lamella while the higher temperature and more predominant melting peak was due to the melting of dominant thicker lamellae (Alfonso, Pedemonte, & Pontzetti, 1979; Carpento, Marsano, Valeti, & Zanardi, 1992; Tan, Su, Luo, & Zhou, 1999). It is assumed that the addition of acetonitrile promotes crystal growth which is confirmed by X-ray scattering (Fig. 4).

3.4. Thermal expansion stability

The thermal expansion stability of each PLA film was determined by measuring the amount of dimensional change with respect to temperature (Table 3 and Fig. 6). Increasing the crystal structure and crystallinity of a polymer can lead to more thermal expansion stability at higher temperatures (Hao & Pintauro, 1999). When molecules in more amorphous regions are subjected to heat they begin to undergo segmental motion which in turn leads to expansion of the material (Selke et al., 2004, chap. 3).

Table 3
Dimensional change of the PLA cast films.

PLA film	Thermal expansion coefficient (µm/°C)	Onset (°C)	Dimensional change (µm)
100M10	15.63	62.54	1546
73MA10	.8194	149.41	217.9
64MA10	.6812	148.06	172
55MA10	.6219	148.86	214.6

Table 4
Haze measurements of the four PLA films.

PLA film	Haze (%)	Transmittance (%)	Clarity (%)
100M10	6.71 ± 2.05^c	94.4 ± 0.39^a	98.66 ± 0.27^a
73MA10	62.52 ± 16.31^b	93.6 ± 1.49^a	49.91 ± 18.34^b
64MA10	100.0 ± 0.00^a	42.88 ± 2.22^b	2.5 ± 0.89^c
55MA10	99.96 ± 0.10^a	22.8 ± 0.96^c	0.18 ± 0.34^c

Different letters within the same column are significantly different (P < 0.05).
Results are expressed as the mean ± SD (n = 9).

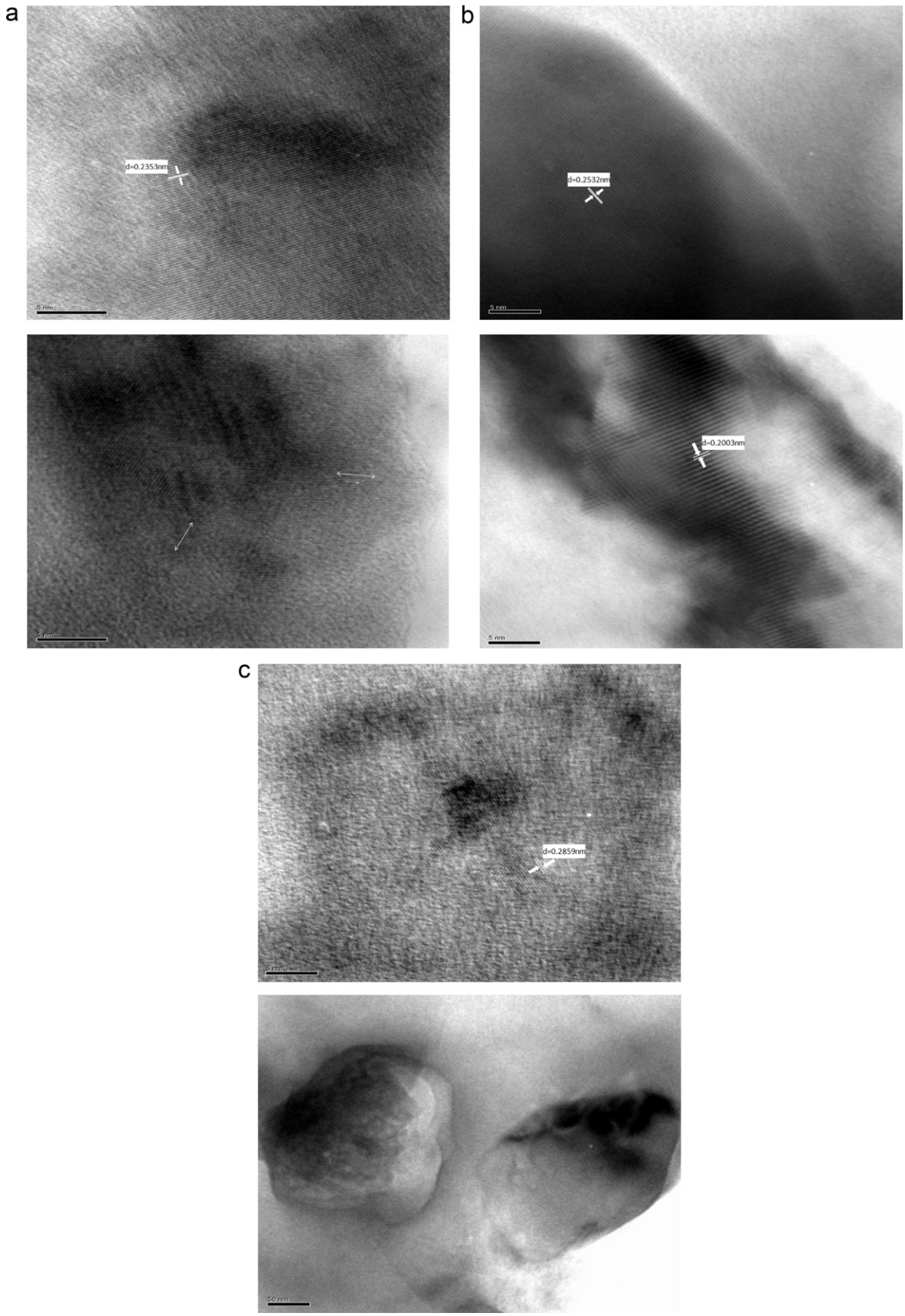

Fig. 7. (a) TEM images of PLA 55MA10; (b) TEM images of PLA 64MA10; and (c) TEM images of PLA 73MA10.

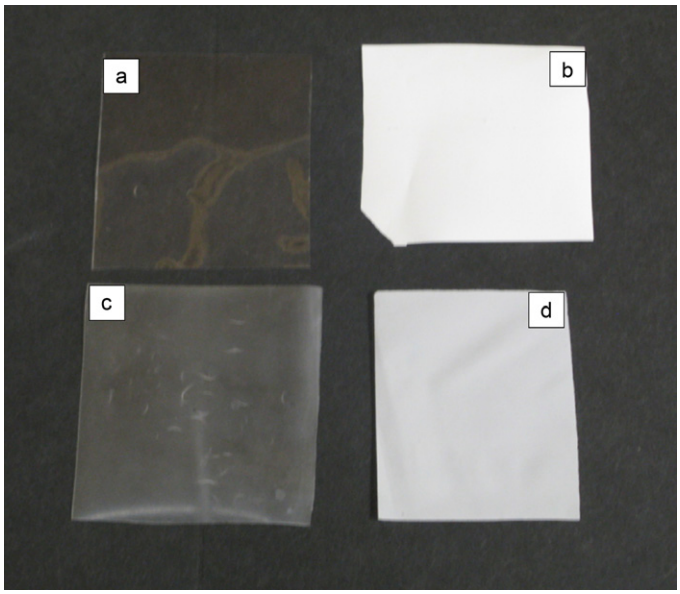

Fig. 8. Photographic images of PLA (a) 100M10; (b) 55MA10; (c) 73MA10; and (d) 64MA10.

Films 55MA10 and 64MA10 had the least dimensional change compared to 100M10 as seen by Byun et al. (2010). Film 55MA10 and 64MA10 also had lower thermal expansion coefficients throughout the whole plasticizer range (Table 3). Film 100M10 showed the most change of all four solvent mixtures with a thermal expansion coefficient of 15.63 μm/°C, dimensional change of 1546 μm and an onset temperature of 62.54 °C (Table 3). These findings were similar to Byun et al. (2010), where the single solvent cast film performed poor when compared to solvent mixtures that included acetonitrile which helped promote crystal formation. 73MA10 had similar melting enthalpies and mechanical properties with 100M10 but, very different thermal expansion stabilities; 73MA10 0.82 μm/°C versus 100M10 15.63 μm/°C. The inclusion of acetonitrile in smaller concentrations gave just enough crystal structure to perform thermally like a crystalline polymer yet ductile enough to behave viscoelastic. Therefore, PLA 55, 64 and 73MA10 were more heat stable than single solvent 100M10 (Table 4).

3.5. HR-TEM

Most of the cast films showed well defined crystalline lattice plane packing (Fig. 7). 55MA10 shows lattice fringes with a *d*-spacing of 0.2353 nm (Fig. 7a). Each dark region indicates a single crystalline structure with the lattice showing among it. Film 64MA10 (Fig. 7b) shows clear lattice fringes with *d*-spacing's of 0.2532 and 0.2003 nm. Areas with tightly packed planes assumed more phase changes took place. Hoogsten et al. (1990) suggested this phase for PLLA as an orthombic unit cell that includes six helices with three fold helical conformation (Hoogsten et al., 1990). Clear, light colored areas beyond the extent of the lattice fringe are the amorphous regions of the polymer. 73MA10 (Fig. 7c) shows a crystal lattice but without multiple lattice planes with a spacing of 0.2859 nm. Graphs from X-ray diffraction (Fig. 4) show that 73MA10 has only one predominant peak at 2θ angle 17°. Film 100M10 did not show a crystalline lattice under high resolution TEM. This was expected as the 100M10 film showed the least crystallinity and poor thermal stability. (Seok & Park, 2009) noticed that as the *d*-spacing increased in polyethylene by the use of clay fillers, the mechanical properties increased. Likewise, the more closely packed the spacing resulted in higher melting temperature and heat of fusion (Seok & Park, 2009).

3.6. Appearance

The appearance of the films differed from very opaque to transparent (Fig. 8). Values for haze, transmittance and clarity of the 10% plasticizer PLA film were taken (Table 2). Not shown are films with plasticizer % ranging from 12 to 20%. 55MA10 and 64MA10 had the highest % haze of all the films at 100% due to its large spherulite size. 100M10 was transparent in appearance and had no haze value. Polymers with higher crystallinity are more opaque than more transparent films. This is due to larger spherulite size in high crystalline polymers scattering light from the different crystal phase changes (Selke et al., 2004, chap. 3). Polymers with smaller sized spherulite's are more transparent and therefore have less light scattering. As expected, the less crystalline 73MA10 and 100M10 had the highest clarity. Because these crystals are so small, less light is scattered and the film appears clear.

4. Conclusion

Film crystallinity was affected by the mixture of different solvents. The increase of crystallinity in film 55MA10 56.94% and 64MA10 52.19%, gave the film more thermal expansion stability 0.6219 μm/°C and 0.6812 μm/°C, respectively. X-ray diffraction confirmed the presence of these solvent induced crystalline structures. 55MA10 and 64MA10 had more crystalline peaks as compared to 100M10 and 73MA10. 100M10 had the least crystallinity (25.95%) therefore it had the highest amount of thermal expansion, 15.63 μm/°C. The films also had a different appearance. The films with higher % crystallinity (55MA10, 64MA10) had the most haze due to larger crystal formation, 99.96 and 100%, respectively. This increase crystallinity resulted in very little clarity with 55MA10 having the least at 0.18%. These films also had lower transmittance and clarity values as compared to 73MA10 and 100M10. The less crystalline films (73MA10, 100M10) having less crystal formation resulted in more clarity, transparency and less haze. Although not as clear as 100M10 with 98.66% clarity, 73MA10 at 49.91% clarity was much better than 64MA10 and 55MA10. Transmittance values of 94.4% for 100M10 and 93.6% for 73MA10 were also higher than the other films. Surprisingly, 73MA10 with nearly the same amount of crystallinity as 100M10 showed similar thermal stability as 55MA10 and 64MA10 with 0.8194 μm/°C thermal expansion. This may be due to the introduction of acetonitrile in small quantities to aid in the formation of crystalline structures that did not fully grow until heating. It appears that 31% crystallinity is the optimum amount of crystallinity to perform ductile enough to have improved elongation and be thermally stable. Films with crystallinity above 31% were brittle whereas films with less crystallinity had poor thermal stability. DSC curves show that 73MA10 had a crystallization peak and an enthalpy of crystallization of 11.25 J/g whereas 55MA10 and 64MA10 did not. Increasing the crystallinity had an effect on the mechanical ability of the film as well. The increased crystallinity made the film perform brittle in nature. 55MA10 with an average tensile strain of 9.13 MPa is much lower than 37.65 MPa of 73MA10 and 52.19 MPa of 100M10. 73MA10 saw ductile performance having more chain mobility as represented by stress–strain curves. Lattice images of the films can be seen by high resolution TEM shows that the presence of acetonitrile promotes different phase changes. Also noticed in the TEM images are the *d*-spacing of each crystal with 73MA10 having wider lattice spacing. From the tests conducted, film 73MA10 was thermally stable compared to 100M10. It also had better elongation (49.36%) than 100M10 (14.24%) and much higher tensile strain than 55MA10 and 64MA10. The objective of this study was to produce a flexible, thermally stable PLA film from solvent mixtures using the solvent casting technique. Developing a film that has the thermal

properties of a crystalline film and yet the flexibility and clarity of an amorphous film can expand the functional uses of a film. This was accomplished with the 73MA10 film.

References

Ahmed, J., Varshney, S., Zhang, J., & Ramaswamy, H. (2009). *Journal of Food Engineering*, *93*, 308.

Alfonso, G. C., Pedemonte, E., & Pontzetti, L. (1979). *Polymer*, *20*, 104.

Bistac, S., & Schultz, J. (1997). *Progress in Organic Coatings*, *31*(4), 347.

Bor-Kuan, C., Hia-Hsu, S., Shu-Chuan, C., & Antonia, F. C. (2010). *Polymer*, *51*, 4667–4672.

Brizzolara, D., Cantow, H. J., Diederichs, K., Keller, E., & Domb, A. (1996). *Journal of Macromolecules*, *29*, 191.

Byun, Y., Kim, Y. T., & Whiteside, S. (2010). *Journal of Food Engineering*, *100*, 239.

Byun, Y., Whiteside, S., Thomas, R., Dharman, M., Hughes, J., & Kim, Y. T. (2011). *Journal of Applied Polymer Science*, in press.

Carpento, L., Marsano, E., Valeti, B., & Zanardi, G. (1992). *Polymer*, *33*, 3865–3872.

Cartier, L., Okihara, T., Ikada, Y., Tsuji, H., Puiggali, J., & Lotz, B. (2000). *Polymer*, *41*, 8909.

De Santis, P., & Kovacs, A. (1968). *Journal of Biopolymers*, *6*(3), 299–306.

Drmright, R., Gruber, P., & Henton, D. (2000). *Advanced Materials*, *12*, 1841.

Fischer, E. W., Sterzel, H. J., Wegner, G., & Kolloid-Zu, Z. (1973). *Polymer*, *251*, 980.

Furuhashi, Y., Wakuda, H., & Yoshie, N. (2006). *Seisan-kenkyu*, *58*, 353.

Garlotta, D. (2001). *Journal of Polymers and the Environment*, *9*, 63.

Haidong, L., Wei, N., Chao, D., Xuesi, C., & Xiangling, J. (2009). *European Polymer Journal*, *45*, 123.

Hao, T., & Pintauro, P. N. (1999). *European Polymer Journal*, *35*, 1023–1035.

Hong, X., Cuiqing, T., & Muhuo, Y. (2006). *Polymer*, *47*, 3922–3928.

Hoogsten, W., Postema, A. R., Pennings, A. J., Ten Brinke, G., & Zugenmaier, P. (1990). *Macromolecules*, *23*, 634.

Huda, M., Yasui, M., Mohri, N., Fulimura, T., & Kimura, Y. (2002). *Materials Science and Engineering A*, *333*, 98.

Jianming, Z., Yongxin, D., Harumi, S., Hideto, T., Isao, N., Shouke, Y., et al. (2005). *Macromolecules*, *38*, 8012–8021.

Jyh-Ping, H., & Sung-Hwa, L. (2005). *European Polymer Journal*, *41*, 1036–1042.

Lim, L. T., Auras, R., & Rubino, M. (2008). *Progress in Polymer Science*, *33*, 820–852.

Mano, J., Gomez-Ribelles, J., Alves, N., & Salmeron-Sanchez, M. (2005). *Polymer*, *46*, 8258.

Michler, G., & Baltá-Calleja, F. (2005). *Mech prop of polymers based on nanostructure and morphology*. Boca Raton: T&F Group.

Miller, E. (1996). *Introduction to plastics and composites*. New York: Marcel Dekker Inc.

Paragkumar, T., Edith, D., & Jean-luc, S. (2006). *Applied Surface Science*, *253*, 2758.

Park, S., Todo, M., Arakawa, K., & Koganemaru, M. (2006). *Polymer*, *47*, 1357.

Pezzin, A., Alberda, G., Zavaglia, C., Ten brinke, G., & Duek, E. (2003). *Journal of Applied Polymer Science*, *88*, 2744.

Pillin, I., Montrelay, N., & Grohens, Y. (2006). *Polymer*, *47*, 4676–4682.

Rhim, J.-W., Hong, S.-I., & Ha, C.-S. (2009). *Food Science and Technology*, *42*, 612–617.

Selke, S., Culter, J. D., & Hernandez, R. (2004). *Plastics packaging* (2nd edition). Cincinnati: Hanser Publications.

Seok, K., & Park, S.-J. (2009). *Journal of Colloid and Interface Science*, *332*, 145–150.

Shujin, W., Jinglin, Y., & Jiungau, Y. (2008). *Carbohydrate Polymers*, *74*, 731–739.

Sin-Lin, Y., Zhi-Hua, W., Yang, W., & Yang, M. (2008). *Polymer Test*, *27*, 957–963.

Slager, J., Brizzolara, D., Cantow, H., & Domb, A. (2005). *Polymers of Advanced Technologies*, *16*, 667.

Sodergard, A., & Stolt, M. (2002). *Progress in Polymer Science*, *27*, 1123.

Stuik, L. C. E. (1978). *Physical ageing in amorphous polymers and other materials*. New York: Elsevier.

Tan, S. S., Su, A. U., Luo, J., & Zhou, E. L. (1999). *Polymer*, *40*, 1223.

Ting, T. L., Xiang, Y. L., & Chaobin, H. (2010). *Polymer*, *51*, 2779–2785.

Xiao, H., Liu, F., & Yeh, J. (2010). *Journal of Applied Polymer Science*, *117*, 2980.

Yamane, H., & Sasai, K. (2003). *Polymer*, *44*, 2569–2575.